Metadata of the chapter that will be visualized in SpringerLink

Book Title	Proceedings of the XVII Conference of the Italian Association for Wind Engineering	
Series Title		
Chapter Title	Influence of Stochastic Load Perturbations on the Performance of a Torsional-Flutter Wind Harvester	
Copyright Year	2024	
Copyright HolderName	The Author(s), under exclusive license to Springer Nature Switzerland AG	
Corresponding Author	Family Name	Caracoglia
	Particle	
	Given Name	Luca
	Prefix	
	Suffix	
	Role	
	Division	
	Organization	Northeastern University
	Address	Boston, MA, 02115, USA
	Email	lucac@coe.neu.edu
	ORCID	http://orcid.org/0000-0002-4783-2600
Abstract	Wind energy technologies are emerging as the need for clean energy resources has considerably increased in the last decade. Apart from horizontal-axis wind turbines, less efficient at the intermediate scales (or meso-scales) and for moderate wind speeds, a competitive alternative is necessary. This alternative is represented by simpler, smaller-size wind-based energy systems, activated by various aeroelastic phenomena. An ongoing investigation on the performance of an aeroelastic harvester, which can efficiently replace meso-scale wind turbines, is discussed. The apparatus exploits the torsional flutter of a streamlined "rigid" blade that rotates about a pre-set axis through a nonlinear torsional spring mechanism that activates post-critical behavior A stochastic model of the apparatus, including output power estimation, has been derived to evaluate relevance of uncertain wind loads, induced by imperfect characterization and simplified load assumptions. Studies are carried out to examine mean square stability.	
Keywords (separated by '-')	Wind Energy Technology - Aeroelastic Harvester - Torsional Flutter - Random Loads - Stochastic Differential Equations	



Influence of Stochastic Load Perturbations on the Performance of a Torsional-Flutter Wind Harvester

Luca Caracoglia^(⊠)

□

Northeastern University, Boston, MA 02115, USA lucac@coe.neu.edu

Abstract. Wind energy technologies are emerging as the need for clean energy resources has considerably increased in the last decade. Apart from horizontal-axis wind turbines, less efficient at the intermediate scales (or meso-scales) and for moderate wind speeds, a competitive alternative is necessary. This alternative is represented by simpler, smaller-size wind-based energy systems, activated by various aeroelastic phenomena. An ongoing investigation on the performance of an aeroelastic harvester, which can efficiently replace meso-scale wind turbines, is discussed. The apparatus exploits the torsional flutter of a streamlined "rigid" blade that rotates about a pre-set axis through a nonlinear torsional spring mechanism that activates post-critical behavior, A stochastic model of the apparatus, including output power estimation, has been derived to evaluate relevance of uncertain wind loads, induced by imperfect characterization and simplified load assumptions. Studies are carried out to examine mean square stability.

Keywords: Wind Energy Technology · Aeroelastic Harvester · Torsional Flutter · Random Loads · Stochastic Differential Equations

1 Introduction

Wind energy is rapidly emerging field because of the need for clean energy. Current technology advancements mainly focus on large-scale, horizontal-axis wind turbines that are less efficient at intermediate scales, i.e., the meso-scales. An interesting alternative is represented by simpler wind-based systems, triggered by various aeroelastic phenomena such as galloping [1], vortex induced vibration [2] and coupled flutter [3, 4]. Caracoglia [5] proposed the use of torsional flutter of a blade-airfoil in Fig. 1, simpler than coupled flutter and other aeroelastic phenomena, to produce energy. The pivot axis (O) in Fig. 1 coincides with the windward position close to stagnation point of the mean flow, from left to right in the figure.

Building on previous studies, a new stochastic model has been recently derived to investigate effects of random perturbations (i.e., load variability) on the performance of the apparatus. Parametric perturbations are employed to describe aeroelastic load variability as a first attempt to replicate imperfect fluid-structure interaction. Examples are three-dimensional flow effects, neglected in standard aeroelastic theory and nonlinear

coupling. Stochastic differential equations are employed to study mean square stability (and output power) of the apparatus, conditional on the value of the wind speed that triggers the instability. This study also preliminarily evaluates output energy and identifies physical properties controlling output power.

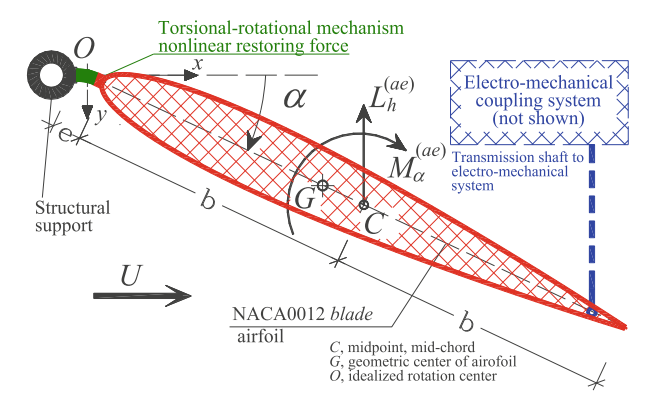


Fig. 1. Cross-sectional schematics of the apparatus and its components.

2 Methodology

A state-space model, based on stochastic differential equations, is employed to study the mean square stability of the apparatus as a function of mean flow speed U. In the reduced-order state-space model, aeroelastic torque is simulated using unsteady load formulation. The triggering mechanism depends on the following quantities: reduced frequency $k_{\alpha} = \omega_{\alpha}b/U$ with ω_{α} [rad/s] angular frequency of linear flapping motion, damping ratio ζ_{α} , generalized inertia ε and cubic stiffness κ . The mean flow speed is U The main one-degree-of-freedom (1DOF) dynamic equation depends on flapping angle (torsional rotation) α and dimensionless time $\tau = t\omega_{\alpha}$:

$$\psi_0 \frac{\mathrm{d}^2 \alpha}{\mathrm{d}\tau^2} + \left(\frac{1.5\varepsilon \eta_{3D}}{k_\alpha} + 2\zeta_\alpha\right) \frac{\mathrm{d}\alpha}{\mathrm{d}\tau} + (\alpha + \kappa \alpha^3) =$$

$$-\varepsilon \eta_{3D} k_\alpha^{-2} \begin{bmatrix} \Phi_0 \left(\alpha + 1.5k_\alpha \frac{\mathrm{d}\alpha}{\mathrm{d}\tau}\right) \\ +1.5\left(\nu_{ae,1} + \nu_{ae,2}\right) + \mu_{ae,1} + \mu_{ae,2} \end{bmatrix} - \Psi\iota$$
(1)

The right-hand side of Eq. (1) shows, within square brackets, the "indicial function" (Wagner) formulation with $\nu_{ae,1}$, $\nu_{ae,2}$, $\mu_{ae,1}$ and $\mu_{ae,2}$ being aeroelastic states; the formulation is corrected for three-dimensional flow effects by quasi-static, simplified correction function $\eta_{3D} = AR/(AR + 2)$ that depends on aspect ratio $AR = \ell/b$ [bladeairfoil's chord half-length b in Fig. 1 vs. depth of the apparatus ℓ]. Quantity $\Phi_0 = 0.5$ denotes the unit-step Wagner function at time $\tau = 0$; parameter $\psi_0 = (1 + 9/8\varepsilon\eta_{3D})$

accounts for non-circulatory flow load effects ("added mass"). Derivation of the equations of motion and aeroelastic states is omitted for the sake of brevity but is available from a previous work [5].

The mass moment of inertia of the apparatus, rotating about O, is $I_{0\alpha}$. On the left-hand side of Eq. (1) an important feature is the nonlinear cubic stiffness term ($\kappa\alpha^3$). The cubic term ensures that the apparatus can efficiently work by achieving a stable post-critical vibration regime. The nonlinear torsional spring mechanism is schematically indicated in Fig. 1 only. The plan is to design a translation spring connected to the chord axis of the rigid apparatus (dashed line in Fig. 1) with cubic properties. This may be achieved, for example, by exploiting the nonlinear geometric properties of a "loose", non-taut cable, aptly designed; an example of this nonlinear stiffness feature has been proposed for the design of "nonlinear energy sinks" [6] that have been used for the passive control of various structures.

On the right-hand side of Eq. (1), $\iota(\tau)$ is a normalized output current. Coupling with an eddy-current power circuit is possible through $\Psi=4b^2(\Phi_{\rm e.m.c.})^2/(\omega_{\alpha}I_{0\alpha}R_C)$, dimensionless electro-mechanical coupling coefficient. $\Phi_{\rm e.m.c}$ is the electro-mechanical coupling coefficient [newton/ampère] due to magnetic induction and interaction of the moving coil with the moving shaft, schematically indicated in Fig. 1. The current ι is found from the relationship $I(\tau)=\iota(\tau)[\Phi_{\rm e.m.c.}2b\omega_{\alpha}/R_C]$, with $I(\tau)$ being the current generated by the eddy-current circuit [in Ampères] and R_C the resistance of the circuit. The properties of the secondary power circuit are found following the steps indicated by Kwon $et\,al.$ [7], i.e., through Faraday's law and induced output current (ι in dimensionless units). Furthermore, the dimensionless equation of the power circuit is derived as $d\iota/d\tau=\lambda_{RL}(d\alpha/d\tau-\iota)$ [5]. The quantity $\lambda_{RL}=R_C/(\omega_{\alpha}L_C)$ is defined as "generalized impedance of the power circuit" with L_C inductance [Henries]; λ_{RL} must be selected to avoid that the electro-magnetic apparatus behaves as a damper that suppresses the flapping [5].

The Itô-type differential equation is derived from Eq. (1), after perturbing the Wagner function needed for airfoil flutter in time domain τ [8], defined as $\Phi(\tau) = c_0 - c_1 \exp[-d_1\tau/k_\alpha] - c_2 \exp[-d_2\tau/k_\alpha]$; with the constant parameters being derived for a NACA0012 cross section as [9]: $c_0 = 1.0$, $c_1 = 0.165$, $c_2 = 0.335$, $d_1 = 0.0455$ and $d_2 = 0.3$.

In this study, random load perturbation is obtained by modifying the reference coefficient d_2 as $d_2=0.3+\Delta_{d2}(\tau)$ with $\Delta_{d2}(\tau)$ being a zero-mean Gaussian white noise of standard deviation σ_{d2} . The reason for exclusively considering randomness in the d_2 parameter is because the second exponential term $\{c_2 \exp[-d_2\tau/k_\alpha]\}$ mainly controls the rapidly varying load variations through $\Phi(\tau)$ function and is mostly responsible for the memory effects. The standard deviation σ_{d2} is selected to replicate a coefficient of variation equal to about 20%, plausible with this type of randomness. Although other perturbations can readily be included in the formulation, they are not considered herein for the sake of simplicity. Further experimental verification would be necessary to better determine their variability.

The randomization $\Delta_{d2}(\tau)$ enables the subsequent derivation of the system of equations below,

$$d\mathbf{w}_{\text{em}} = \mathbf{q}_{\text{NL},\Delta}(\mathbf{w}_{\text{em}})d\tau + \sqrt{2\pi}\mathbf{Q}_{\text{L},\Delta}\mathbf{w}_{\text{em}}dB(\tau)$$
 (2)

where \mathbf{W}_{em} is the state vector, $\mathbf{q}_{\mathrm{NL},\Delta}$ is a nonlinear drift vector, $\mathbf{Q}_{\mathrm{L},\Delta}$ is a diffusion matrix, $B(\tau)$ is a scalar Wiener noise of dimensionless time τ that is used to represent the randomness of $\Delta_{d2}(\tau)$. Turbulence effects are neglected.

The state vector has seven variables and includes physical states (rotation and its derivative), aeroelastic states and dimensionless current $\iota(\tau)$; \mathbf{W}_{em} reads

$$\mathbf{W}_{em}(\tau) = \left[\alpha(\tau), d\alpha(\tau)/d\tau, \nu_{ae,1}(\tau), \nu_{ae,2}(\tau), \mu_{ae,1}(\tau), \mu_{ae,2}(\tau), \iota(\tau) \right]^T$$
(3)

The non-zero elements of the 7-by-7 diffusion matrix $\mathbf{Q}_{L,\Delta}$ in Eq. (2) are:

$$(\mathbf{Q}_{L,\Delta})_{4,2} = (\mathbf{Q}_{L,\Delta})_{6,1} = \sigma_{d2} k_{\alpha}^{-1} c_2, \quad (\mathbf{Q}_{L,\Delta})_{6,6} = -\sigma_{d2} k_{\alpha}^{-1}$$
 (4)

Coefficients in Eq. (4) are constant and depend on the random load perturbation $\Delta_{d2}(\tau)$ through standard deviation σ_{d2} . The drift function in Eq. (2) is nonlinear:

$$\mathbf{q}_{\text{NL},\Delta}(\mathbf{W}_{\text{em}}) = \begin{cases} W_{\text{em},2} \\ 8/[8 + 9\varepsilon\eta_{3D}] \tilde{\Pi}_{\mathbf{W}_{\text{em}}}(\mathbf{W}_{\text{em}}) \\ d_1[c_1 W_{\text{em},2} - k_{\alpha}^{-1} W_{\text{em},3}] \\ [d_{2,m} + \pi \sigma_{d2}^2][c_2 W_{\text{em},2} - k_{\alpha}^{-1} W_{\text{em},4}] \\ k_{\alpha}^{-1} d_1[c_1 W_{\text{em},1} - W_{\text{em},5}] \\ k_{\alpha}^{-1} \left[\overline{d}_2 + \pi \sigma_{d2}^2 \right] [c_2 W_{\text{em},1} - W_{\text{em},6}] \\ \lambda_{RL}[W_{\text{em},2} - W_{\text{em},7}] \end{cases}$$
(5)

Equation (5) is presented as a 7-by-1 functional $\mathbf{q}_{\mathrm{NL},\Delta}(\mathbf{W}_{\mathrm{em}})$; the last equation also describes electro mechanical coupling through $W_{\mathrm{em},2} = \mathrm{d}\alpha/\mathrm{d}\tau$ and $W_{\mathrm{em},7} = \iota(\tau)$. The nonlinear function of the second – row element is:

$$\widetilde{\Pi}_{\mathbf{W}_{em}}(\mathbf{W}_{em}) = -\binom{W_{em,1}}{+\kappa W_{em,1}^3} - \left(\frac{3\varepsilon\eta_{3D}}{2k_{\alpha}} + 2\zeta_{\alpha}\right) W_{em,2} \\
-\frac{\varepsilon\eta_{3D}}{k_{\alpha}^2} \begin{bmatrix} \Phi_0 \left(W_{em,1} + \frac{k_{\alpha}W_{em,2}}{2/3}\right) + W_{em,5} + W_{em,6} \right] - \Psi W_{em,7} \\
\frac{W_{em,3} + W_{em,4}}{2/3} + W_{em,5} + W_{em,6} \end{bmatrix} - \Psi W_{em,7}$$
(6)

In Eqs. (4) and (5) the Wong and Zakai [10] correction terms are included. Finally, Eq. (2) is combined with Eqs. (4–6) and solved numerically. The Euler numerical integration scheme [11] is employed to solve Eq. (2) several times, i.e., by defining a "population of realizations" and collecting each solution or \mathbf{W}_{em} as a function of time. It is noted that initial random vector $\mathbf{W}^{(0)}_{em}$ at $\tau=0$ is also needed; initial conditions are imposed by assuming random initial rotation different from zero, expressed as a random, Gaussian, scalar angle perturbation $W_{em,1}$ with given properties and identically zero initial conditions for other states, i.e., $\mathbf{W}^{(0)}_{em} = [\alpha_0, 0, ..., 0]^T$. The ensemble of the solutions is collected and later utilized to examine stability.

The second Moment Lyapunov Exponent (MLE) $\Lambda_{\Xi}(2)$ is used to study the dynamic stability. The second-moment Lyapunov exponent [12] examines the propensity of a stochastic dynamic system to become unstable in terms of mean squares (variances and

co-variances). This is scalar quantity that measures the rate of change of the "slow time dynamics" and evaluates the state as time tends to infinity; in other words, it can be assimilated to the total damping of the system at steady state after an initial, transitory stage.

A negative value of $\Lambda_{\Xi}(2)$ is needed to ensure mean-square stability; therefore, $\Lambda_{\Xi}(2) > 0$ yields an apparatus that produces energy. The stability limit varies as a function of wind speed. By varying U, both incipient and post-critical conditions are evaluated. Relevance is attributed to the output current $\iota = w_{\rm em,7}$ that is extracted from the secondary system and, consequently the output power.

The $\Lambda_{\Xi}(2)$ quantity is found by solving Eq. (2) using numerical integration; $\Lambda_{\Xi}(2)$ is approximated as:

$$\Lambda_{\Xi}(2) \approx \log_e \left(\mathbb{E} \left[\|\Xi\|^2 \right] \right) / \tau_j$$
 (7)

where $\Xi(\tau) = [\alpha(\tau), d\alpha(\tau)/d\tau]^T$ is a suitable, dynamic sub-vector of \mathbf{W}_{em} and τ_j a discrete time, needed in conjunction with step-by-step integration. The time index j is taken sufficiently large, i.e., tending to infinity. Discussion on the validity of Eq. (7) to approximate the limit may be found in a previous study [13]. Accuracy in the calculation of Eq. (7) is achieved by reducing the time step for numerical integration of Eq. (2) and selecting a sufficiently large sample of solutions to derive expectations in Eq. (7).

3 Results

Numerical solution of the stochastic Eq. (2) in a post-critical regime is studied. The main properties of the apparatus, selected in this study, are: damping ratio ζ_{α} , electromechanical coupling coefficient Ψ , generalized impedance λ_{RL} and aspect ratio AR. The following reference quantities are set: $\zeta_{\alpha} = 0.25\%$, $\Psi = 0.01$, $\lambda_{RL} = 0.75$, AR = 10, and $\kappa = 100$ in dimensionless units.

Three basic configurations of the apparatus are investigated:

- Type 0 with $\omega_{\alpha}/2\pi = 0.25$ Hz, b = 0.25 m, $I_{0\alpha}/\ell = 20$ kg-m²/m;
- Type I with $\omega_{\alpha}/2\pi = 0.20$ Hz, b = 0.25 m, $I_{0\alpha}/\ell = 40$ kg-m²/m;
- Type 2 with $\omega_{\alpha}/2\pi = 0.10$ Hz, b = 0.50 m, $I_{0\alpha}/\ell = 300$ kg-m²/m.

These configurations are derived to achieve minimum operational conditions at mean flow speed between 10 m/s and 15 m/s [5, 13] and, at the same time, to be relatively compact (small b) and have the potential for practical implementation and installation on building roofs.

Numerical investigations examine both a variation in the random load perturbation $\Delta_{d2}(\tau)$, with zero mean and standard deviation σ_{d2} variable between 0.07 and 0.10. Moreover, because of the perceived nonlinear uncertainty perturbation in Eq. (6), effects of the initial random conditions are evaluated, i.e., an initial "flapping" angle $[\alpha_0]$ with zero mean and standard deviation equal to both $\sigma_{\alpha0} = 1.8$ deg (small deviations) and $\sigma_{\alpha0} = 18.0$ deg (large deviations). An initial angle α_0 is always needed to trigger instability and cause the system to store energy.

Figure 2 illustrates an example of the numerical results for the three basic apparatuses with AR = 10; this large AR value is considered to simulate negligible three-dimensional flow effects. In this figure, the designation "Type" is abbreviated as "Ty.", with 0,1,2 indicating the numeral identifier.

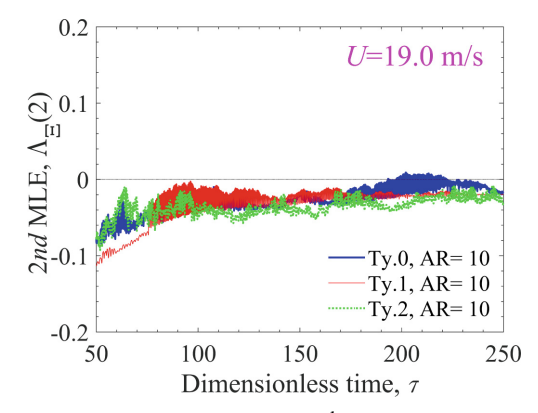


Fig. 2. Mean-square dynamic stability analysis via 2^{nd} MLE [$\Lambda_{\Xi}(2)$] at flow speed U = 19.0 m/s for an apparatus with aspect ratio AR = 10, $\sigma_{d2} = 0.07$ and $\sigma_{\alpha0} = 1.8$ deg (small initial amplitude).

Figure 2 demonstrates that, as a first example, at the stated wind speed $\Lambda_\Xi(2)$ of all three systems are tending to an unstable asymptote, with $\Lambda_\Xi(2)>0$, and can trigger energy conversion. In fact, the trends of $\Lambda_\Xi(2)$ found by Eq. (7) numerically exhibit a progressively positive value despite an initial negative trend of Type 2. The introduction of randomness in the aeroelastic load with Δ_{d2} having moderate variability and a standard deviation $\sigma_{d2}=0.07$. The flow speed at which the system transitions from stable to unstable is above U=15 m/s, which is a plausible estimate of the stability threshold [5] in the absence of random aeroelastic load, suggesting that load variability has a stabilizing effect. This remark indicates that variability in the loads produces a delay in the onset of the flutter vibration and may be detrimental to the efficiency of the apparatus.

Figure 3 illustrates the stability analysis of the Type-2 apparatus with AR = 10 but considers the influence of initial conditions on the stability. In this case, the objective is to study potential nonlinear effects in Eq. (6) (cubic nonlinearity in state variable $W_{\rm em,1}$) through initial state α_0 perturbation. Large initial amplitudes are imposed with zeromean α_0 but standard deviation $\sigma_{\alpha 0}=18.0$ deg, possibly unrealistic since the vibration is evaluated at angles close to the stall for this type of airfoils and for which the aeroelastic load through Wagner function becomes unrealistic and a different formulation is needed [14]. The stability limit is examined in Fig. 3 at a mean flow speed U lower than the previous figure.

The trend exhibited by $\Lambda_{\Xi}(2)$ at large τ in Fig. 3 appears to be negative, at least for Type-2 apparatus, already at U=17.8 m/s; the situation persists for U>17.8 m/s. This observation suggests that, contrary to Fig. 2, stability is negatively affected by larger-amplitude initial conditions and that larger α_0 would be needed to ensure that the apparatus is active and converts flow kinetic energy into electrical energy.

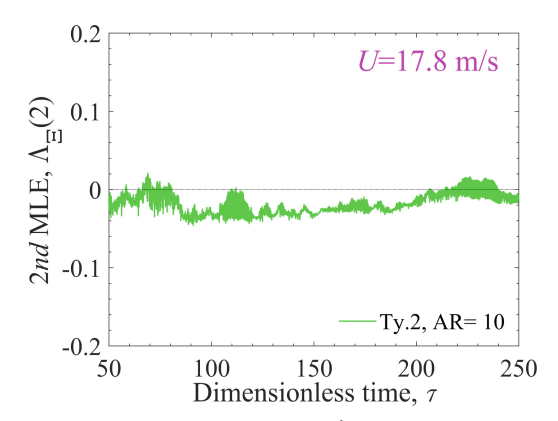


Fig. 3. Mean-square dynamic stability analysis via 2^{nd} MLE [$\Lambda_{\Xi}(2)$] at flow speed U=17.8 m/s for Type-2 apparatus with aspect ratio AR = 10, $\sigma_{d2}=0.07$ and $\sigma_{\alpha0}=18.0$ deg (large initial amplitude).

Figure 4 depicts the time evolution of $\Lambda_{\Xi}(2)$ for all three apparatuses for small initial flapping ($\sigma_{\alpha 0} = 1.8$ deg) at triggering, when the random perturbation of the load parameter Δ_{d2} has a standard deviation 1.41 times larger than the first scenario (Fig. 2). The stability is studied at U = 18.8 m/s very close to U = 19.0 m/s in Fig. 2.

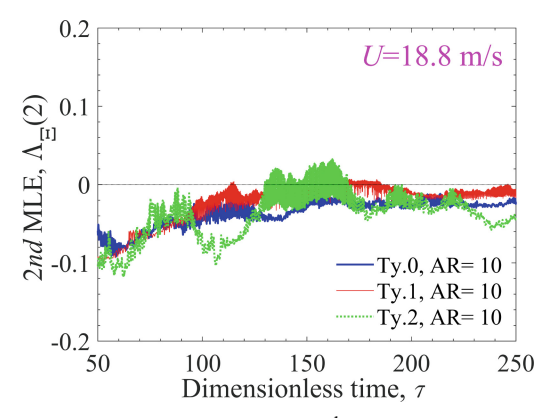


Fig. 4. Mean-square dynamic stability analysis via 2^{nd} MLE [$\Lambda_{\Xi}(2)$] at flow speed U = 18.8 m/s for an apparatus with aspect ratio AR = 10, $\sigma_{d2} = 0.10$ and $\sigma_{\alpha0} = 1.8$ deg.

The trends of in Fig. 4 are very similar to the ones observed earlier. More pronounced fluctuations of $\Lambda_{\Xi}(2)$ about the zero horizontal axis are noted, prior to the asymptotic limit. This result indicates a possibly small influence of σ_{d2} on the overall stability. Nevertheless, numerical integration issues cannot be excluded; they may be related to the selection of the sample size (200 realizations) used to solve Eq. (2) (time step $\Delta \tau = 1\text{E-4}$) and to find the MLE by Eq. (7) and ensemble averaging.

In any case, the choice of the time "limit" $\tau = \tau_j = 250$ seems appropriate since it coincides with 40 periods of torsional oscillation at angular frequency ω_{α} , approximately

coincident with flutter angular frequency. This aspect is examined in Fig. 5, where the estimation of Eq. (7) is extended to $\tau = \tau_j = 500$; the same asymptotic trends are already discernible for all the three apparatuses at about $\tau = 200$, excluding the need for continuing the numerical integration beyond the value used in Fig. 4 and in the previous cases.

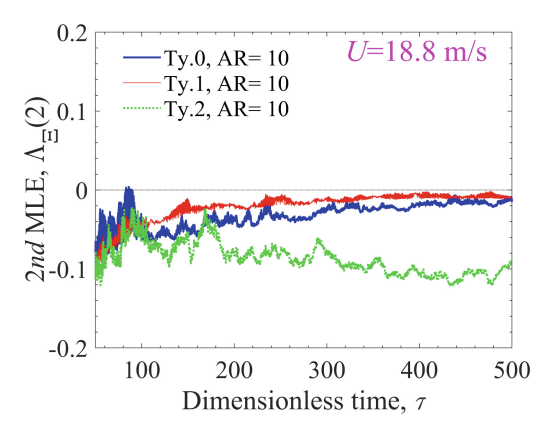


Fig. 5. Extended-time mean-square stability analysis [$\Lambda_{\Xi}(2)$] at flow speed U=18.8 m/s for an apparatus with aspect ratio AR = 10, $\sigma_{d2}=0.10$ and $\sigma_{\alpha0}=1.8$ deg.

4 Conclusions

Numerical study results indicate that introduction of variability in the aeroelastic load may be detrimental and may postpone flutter occurrence, requiring a mean flow speed of magnitude 20% larger than the scenario in the absence of load modeling uncertainty. This result requires further investigation also because the estimation of MLE by ensemble averaging is affected by the choice of the time step used for integration of the stochastic differential equation [Eq. (2)]. Additional studies should be conducted to confirm the influence of uncertainty in the aeroelastic loads, as a function of the standard deviation of the random parameters in the Wanger function. The final goal of this research is the identification and exclusion of low-efficiency operational regimes by rigorous probabilistic analysis. Anticipated results will open new avenues that will be employed in conjunction with future wind tunnel verification.

Acknowledgments. This material is based in part upon work supported by the National Science Foundation (NSF) of the United States of America, Award CMMI-2020063. Any opinions, comments or conclusions are those of the author and do not necessarily reflect the views of the NSF or any other organization.

References

 Abdelkefi, A., Nayfeh, A.H., Hajj, M.R.: Design of piezoaeroelastic energy harvesters. Nonlinear Dyn. 68(4), 519–530 (2012)

- Bernitsas, M.M., Raghavan, K., Ben-Simon, Y., Garcia, E.M.H.: VIVACE (Vortex Induced Vibration Aquatic Clean Energy): a new concept in generation of clean and renewable energy from fluid flow. J. Offshore Mech. Arct. Eng. 130(4), 041101 (2008)
- 3. Shimizu, E., Isogai, K., Obayashi, S.: Multiobjective design study of a flapping wind power generator. J. Fluids Eng. ASME **130**(2), 021104 (2008)
- 4. Pigolotti, L., Mannini, C., Bartoli, G., Thiele, K.: Critical and post-critical behaviour of two-degree-of-freedom flutter-based generators. J. Sound Vib. 404, 116–140 (2017)
- Caracoglia, L.: Modeling the coupled electro-mechanical response of a torsional-flutter-based wind harvester with a focus on energy efficiency examination. J. Wind Eng. Ind. Aerodyn. 174, 437–450 (2018)
- Vakakis, A.F., Gendelman, O.V., Bergman, L.A., McFarland, D.M., Kerschen, G., Lee, Y.S.: Nonlinear targeted energy transfer in mechanical and structural systems (Volumes I and II). Springer Science, New York, New York, USA (2008). https://doi.org/10.1007/978-1-4020-9130-8
- Kwon, S.-D., Park, J., Law, K.: Electromagnetic energy harvester with repulsively stacked multilayer magnets for low frequency vibrations. Smart Mater. Struct. 22(5), 055007 (2013)
- 8. Bisplinghoff, R.L., Ashley, H., Halfman, R.L.: Aeroelasticity. Dover Publications Inc., Mineola, NY, USA (1955)
- 9. Jones, R.T.: The unsteady lift of a finite wing. Technical Note 682. NACA (1939)
- Wong, E., Zakai, M.: On the relation between ordinary and stochastic differential equations. Int. J. Eng. Sci. 3, 213–229 (1965)
- 11. Kloeden, P.E., Platen, E., Schurz, H.: Numerical Solution of Stochastic Differential Equations through Computer Experiments. Springer-Verlag, Berlin-Heidelberg, Germany (1994)
- Xie, W.-C.: Dynamic Stability of Structures. Cambridge University Press, New York, NY, USA (2006)
- Caracoglia, L.: An Euler-Monte Carlo algorithm assessing Moment Lyapunov Exponents for stochastic bridge flutter predictions. Comput. Struct. 122, 65–77 (2013)
- 14. Dunn, P., Dugundji, J.: Nonlinear stall flutter and divergence analysis of cantilevered graphite/epoxy wings. AIAA J. **30**(1), 153–162 (1992)